Therapeutic targeting of BRD4 in head neck squamous cell carcinoma

Yaping Wu[1,2,4] , Yanling Wang[1,4], Pengfei Diao[1], Wei Zhang[1,3], Jin Li[1,2,3] , Han Ge[1], Yue Song[1], Zhongwu Li[2], Dongmiao Wang[2], Laikui Liu[3], Hongbing Jiang[2], Jie Cheng[1,2*]

Supplementary Figure legends

Figure S1. The expression levels of BRD2 and BRD3 mRNA (log2-transformed) are compared between HNSCC samples and normal counterparts in multiple patient cohorts

A. The original data were retrieved from TCGA and Oncomine database and then plotted. Y-axis represents the median intensity, 25th and 75th percentile data. Student's *t* test or Mann-Whitney U test as appropriate. ns, not significant, *$P < 0.05$, **$P < 0.01$.

B-C. The mRNA expression of BRD2 (B) and BRD3 (C) was comparable between the HNSCC and paired normal tissues. The height of column represents the fold change (log2-transformed) in BRD2 and BRD3 mRNA expression in our cohort of 65 patients with HNSCC. Paired *t* test; ns, not significant.

D. Relative expression of BRD2 and BRD3 mRNA (Log2-transformed) was comparable among TCGA-HNSC subgroups stratified by pathological grades. Y-axis represents the median intensity, 25th, and 75th percentile data. ANOVA test; ns, not significant.

E. Overall survival of TCGA-HNSC patients stratified with high or low expression of BRD2, BRD3 and BRD4 mRNA (median values as cutoff) were estimated by Kaplan-Meier method and compared with Log-rank test.

Figure S2. Genetic alternations of BRD2, BRD3 and BRD4 in TCGA-HNSCC dataset

A-D. Genetic alternations of BRD2, BRD3 and BRD4 were detected in TCGA-HNSCC dataset via cBioPortal platform (http://www.cbioportal.org).

Figure S3. BRD4 overexpresses in HNSCC cell lines and tissues

A. Endogenous BRD4 protein expression was measured in a panel of HNSCC cell lines as compared to normal oral epithelial (HOK). Representative images of western blot were shown from 3 independent experiments.

B-C. The protein abundance of BRD4 in 40 pairs of fresh HNSCC samples and adjacent non-tumour epithelial was determined by western blot. Representative images of western blot were shown from 16 pairs of samples (**B**). Quantification data of BRD4 protein were shown (**C**). Paired *t* test, $*P < 0.05$, $**P < 0.01$.

Figure S4. BRD4 knockdown enhances the chemotherapeutic sensitivity in HNSCC

A-B. Cell viability was significantly impaired in BRD4-knockdown cells treated with 5-FU (2.5μg/ml) or cisplatin (2.5μg/ml) alone than those treated with vehicle. Student's *t* test, $*P < 0.05$, $**P < 0.01$.

Figure S5. BRD4 knockdown inhibited tumorsphere formation of HNSCC cells in vitro

A-B. The ability of tumorsphere formation was significantly reduced in shBRD4-2-transfected cells relative to cells with control shRNA. Scale bar: 50μm. Student's *t* test, $*P < 0.05$; $**P < 0.01$.

Figure S6. BRD4 overexpression promotes cell proliferation, migration and invasion in HNSCC cell

A. Increased BRD4 protein was confirmed by western blot in HEK293T and HN6 cells with stable BRD4 overexpression. Representative images of western blot were shown from 3 independent experiments.

B. Cell proliferation was remarkably accelerated following BRD4 overexpression as assayed by MTT viability and colony formation. Student's *t* test, $*P < 0.05$, $**P < 0.01$.

C-D. Cell migration and invasion abilities of HN6 with or without BRD4 overexpression were measured by wound healing and transwell invasion assays. Student's *t* test, $*P < 0.05$, $**P < 0.01$.

Figure S7. BRD4 inhibitors decrease c-Myc expression in HNSCC in qRT-PCR assays (GAPDH was used as loading control)

A. The chemical structures of JQ1 (left panel) and OTX015 (right panel).

B. The values of IC50 (72h) of JQ1 and OTX015 in four types of cells were listed.

C. Endogenous c-Myc protein was inhibited by JQ1 treatment (0.5μM, upper panel). Endogenous c-Myc protein was inhibited by OTX015 in a dosage-dependent manner in Cal27 and Fadu cells (lower panel). Representative images of western blot were shown.

D. The mRNA levels of c-Myc were significantly decreased following OTX015 treatment (0.5μM) for indicated time. GAPDH was used as loading control. ANOVA analyses, $*P < 0.05$, $**P < 0.01$.

E. The mRNA levels of BRD4 weren't affected following JQ1 (left panel) or OTX015 (right panel) treatments (0.5μM) for indicated time. GAPDH was used as loading control. ANOVA analyses, $*P < 0.05$, $**P < 0.01$.

Figure S8. BRD4 inhibitors decrease c-Myc expression in HNSCC in qRT-PCR assays (18sRNA was used as loading control)

A-B. The mRNA levels of c-Myc were significantly decreased following JQ1 (**A**) or OTX015 (**B**) treatment (0.5μM) for indicated time. 18sRNA was used as loading control. ANOVA analyses, $*P < 0.05$, $**P < 0.01$.

C-D. The mRNA levels of BRD4 weren't affected following JQ1 (**C**) or OTX015 (**D**) treatments (0.5μM) for indicated time. 18sRNA was used as loading control. ANOVA analyses, $*P < 0.05$, $**P < 0.01$.

Figure S9. BRD4 inhibitors inhibit cell proliferation, induce cell apoptosis and enhance chemotherapeutic sensitivity in HNSCC

A-B. Cell proliferation of Cal27 or Fadu was significantly reduced upon treatment with JQ1 as measured by

MTT assay. ANOVA analyses, *$P < 0.05$, **$P < 0.01$.

C-D. Cell proliferation of Cal27 or Fadu were significantly reduced upon treatment with OTX015 as measured by MTT assay. ANOVA analyses, *$P < 0.05$, **$P < 0.01$.

E. Increased percentages of apoptotic cells were observed following JQ1 treatment as assayed by Annexin V-PI staining. Representative images were shown.

F-G. Increased percentages of apoptotic cells were observed following OTX015 treatment as assayed by Annexin V-PI staining. Representative images were shown. Student's *t* test, *$P < 0.05$; **$P < 0.01$.

H. Cell viability was more significantly reduced in cells treated with JQ1 (0.5μM) plus 5-FU (2.5μg/ml) or cisplatin (2.5μg/ml) as compared to those treated with single agent. ANOVA analyses, *$P < 0.05$, **$P < 0.01$.

Figure S10. JQ1 treatment inhibits tumor growth in a HNSCC xenograft model

A. Experimental scheme of HNSCC xenograft model. Cal27 or Fadu cells were inoculated subcutaneously into nude mice to establish a xenograft model. Once tumor volume reached appropriate $100mm^3$, these mice were randomly divided into two groups (n=6 for each group), either treated with JQ1 (50mg/kg/day) or vehicle for 15days.

B-C. Tumor volumes of Cal27 or Fadu xenograft were measured every three days following treatment initiation. Final weight of tumor masses harvested from JQ1-treated or control animals was compared (right panel). Student's *t* test, *$P < 0.05$, **$P < 0.01$.

D-E. Representative immunohistochemical staining of c-Myc, Ki67 and Cleaved caspase3 in Cal27 (**D**) and Fadu (**E**) derived xenograft samples treated with JQ1 or vehicle. Scale bar: 50μm.

Figure S11. Genomic transcriptional profiling identifies JQ1-regualted genes in HNSCC

A. The top upregulated (red) and downregulated (green) genes with more than 2-fold affected by JQ1 in

Cal27 and Fadu cells were clustered and shown in heatmap.

B. GSEA analyses revealed that genes regulated by JQ1 in Cal27 cells were significantly enriched in GO categories: regulation of cell proliferation and growth.

C. Several gene candidates downregulated by JQ1 were aberrantly overexpressed in cancer samples in TCGA-HNSCC dataset. This analysis was performed using online platform http://gepia.cancer-pku.cn/. Student's *t* test, **P* < 0.05, ***P* < 0.01.

D. Among 52 top downregulated genes, expression status of 4 genes (median values as cutoff) were found to be significantly associated with overall survival in TCGA-HNSCC dataset (Log-rank test).

Figure S12. The mRNA expression changes of ten candidate genes upon JQ1 treatment are validated by qRT-PCR assays

A-B. The mRNA levels of ten gene candidates were determined by qRT-PCR assays and the c-Myc was selected as a positive control. 18sRNA was utilized as loading control. Student's *t* test, $^{\#}$ not significant, **P* < 0.05, ***P* < 0.01.

Figure S13. JQ1-downregulated (A) or upregulated (B) genes are significantly enriched in multiple cancer-related pathways as assessed by KEGG analyses

Figure S14. JQ1-downregulated (A) or upregulated (B) genes are significantly enriched in several cancer-related pathways as assessed by GO analyses

Figure S15. Overlaps of JQ1-regulated genes in HNSCC cells and multiple myeloma cells or neuroblastoma cells

A. The overlaps of JQ1-regulated genes (>2 fold change) in HNSCC cells (Cal27 and Fadu) and multiple

myeloma cells (KMS11, MM1.S and OPM1, data from GSE31365) were shown with venn diagram.

B. The overlaps of JQ1-regulated genes (>2 fold change) in HNSCC cells (Cal27 and Fadu) and neuroblastoma cells (Be2C and Kelly, data from GSE43392) were shown with venn diagram.

Figure S16. Flowchart illustrating detailed protocol to generate 4-gene based JQ1-regulated prognostic signature

Figure S17. Expression changes of 4 genes upon JQ1 treatment or BRD4 knockdown are measured by qRT-PCR assays

A-B. The mRNA levels of FRMD5, MXD4, PITPNM3 and TRIB3 in Cal27 (**A**) or Fadu (**B**) were detected by qRT-PCR upon JQ1 treatment. 18sRNA was used as loading control. Student's *t* test, **P* < 0.05, ***P* < 0.01.

C-D. The mRNA levels of FRMD5, MXD4, PITPNM3 and TRIB3 in Cal27 (**C**) and Fadu (**D**) were detected by qRT-PCR upon BRD4 knockdown. 18sRNA was used as loading control. Student's *t* test, **P* < 0.05, ***P* < 0.01.

Figure S18. Risk score distribution in samples and its prognostic utility in TCGA-HNSCC cohort and two independent GEO cohorts

A-C. Distribution of prognostic risk score and expression of each mRNA in TCGA-HNSCC, GSE41613 and GSE42743 cohorts (upper and middle panels).

D. The optimal cutoff value for the prognostic risk score was generated by ROC curve using TCGA-HNSCC as training cohort.

E-F. The sensitivity and specificity of this prognostic risk score were also confirmed in GSE41613 (testing) and GSE42743 (validation) cohorts.

Table S1. Associations between BRD4 mRNA and clinicopathological parameters in primary fresh HNSCC samples

Clinicopathological parameters	Cases	BRD4		*P*-values
		Low	High	
Gender	65	33	32	>0.9999
Male	39	20	19	
Female	26	13	13	
Age				0.7944
≤60	21	10	11	
＞60	44	23	21	
Smoking				0.6059
No	42	20	22	
Yes	23	13	10	
Alcohol use				0.2600
No	48	22	26	
Yes	17	11	6	
Tumor size				**0.0414**
T1-T2	41	25	16	
T3-T4	24	8	16	
Pathological grade				0.4586
Ⅰ	35	16	19	
Ⅱ-Ⅲ	30	17	13	
Cervical node metastasis				**0.0225**
N(0)	40	25	15	
N(+)	25	8	17	
Clinical stage				0.3248
Ⅰ-Ⅱ	33	19	14	
Ⅲ-Ⅳ	32	14	18	

Median value of BRD4 mRNA was used as cutoff to stratify patients into BRD4 low or high subgroups.

The number in bold indicate statistical significance with *P*-values less than 0.05.

Table S2. BRD4 protein expression in HNSCC and normal oral mucosa.

	BRD4 expression			
	Negative	**Low**	**High**	***P*-values**
Normal oral mucosa	5	12	7	<0.0001
HNSCC	0	31	72	

Table S3. Associations between BRD4 protein expression and clinicopathological parameters in primary HNSCC samples

Clinicopathological parameters	Cases	BRD4		*P*-values
		Low	High	
Gender	103	31	72	0.6669
Male	59	19	40	
Female	44	12	32	
Age				0.3351
≤60	28	6	22	
＞60	75	25	50	
Smoking				0.6059
No	73	22	51	
Yes	30	9	21	
Alcohol use				0.617
No	78	25	53	
Yes	25	6	19	
Tumor size				**0.0376**
T1-T2	71	26	45	
T3-T4	32	5	27	
Pathological grade				**0.0344**
Ⅰ	58	17	41	
Ⅱ	34	14	20	
Ⅲ	11	0	11	
Cervical node metastasis				0.281
N(0)	61	21	40	
N(+)	42	10	32	
Clinical stage				0.5243
Ⅰ-Ⅱ	51	17	34	
Ⅲ-Ⅳ	52	14	38	

The number in bold indicate statistical significance with *P*-values less than 0.05.

Table S4. Univariate and multivariate survival analyses for patients with primary HNSCC.

Variable	Univariate survival analysis			Multivariate survival analysis		
	Hazard ratio	95% CI	*P*-value	Hazard ratio	95% CI	*P*-value
Gender (male, female)	1.117	0.597–2.093	0.729	0.966	0.441–2.115	0.931
Smoking (No, Yes)	1.090	0.554–2.146	0.803	1.372	0.413–3.123	0.806
Alcohol use (No, Yes)	1.035	0.506–2.120	0.924	1.106	0.377–3.241	0.854
Age (≤60, >60)	1.204	0.645–2.248	0.560	1.476	0.759–2.870	0.251
Tumorsize (T1-T2, T3-T4)	0.733	0.386–1.392	0.343	1.120	0.416–3.016	0.822
Pathological grade (I, II-III)	0.705	0.379–1.312	0.270	0.764	0.328–1.779	0.532
Cervical nodal metastasis (N0, N+)	0.596	0.320–1.109	0.102	0.848	0.324–2.216	0.736
Clinical stage (I-II, III-IV)	0.696	0.371–1.303	0.257	0.776	0.287–2.102	0.618
BRD4 expression (low, high)	0.381	0.168–0.865	**0.021**	0.357	0.145–0.882	**0.026**

The numbers in bold indicate statistical significance with *P*-values less than 0.05.

Table S5. BRD4 expression pattern in samples harvested from different stages in 4NQO-induced HNSCC model.

	BRD4 expression		*P*-value
	Negative/Low	High	
Healthy mucosa	2	4	**0.0385**
Hyperplasia	1	5	
Dysplasia/carcinoma in situ	4	2	
Carcinoma	7	1	

Table S6. Univariate and Multivariate Cox-regression analyses of risk score and clinicopathological parameters in TCGA-HNSCC.

Variables	Univariate analyses		Multivariate analyses	
	HR [95% CI]	*P*	HR [95% CI]	*P*
Combined cohort				
Age (≥60, <60)	1.291(0.981-1.700)	0.069		N/A
Gender (male, female)	0.754(0.566-1.004)	0.054		N/A
Smoking history category (≥3, <3)	0.802(0.606-1.062)	0.123		N/A
Alcohol use (Yes, No)	0.978(0.734-1.304)	0.880		N/A
Tumor size (T3-T4, T1-T2)	1.569(1.143-2.153)	**0.005**	1.751(0.991-3.093)	0.054
Pathological grade (III-IV, I-II)	1.743(1.177-2.580)	**0.006**	1.418(0.791-2.544)	0.241
Cervical nodal metastasis (N+, N0)	1.383(1.039-1.842)	**0.026**	1.213(0.834-1.766)	0.312
Clinical stage (III-IV, I-II)	1.257(0.901-1.753)	0.178	0.571(0.334-0.976)	**0.040**
Risk score (High, Low)	2.247(1.709-2.955)	**<0.001**	2.070(1.518-2.822)	**<0.001**

HR, hazard ratio; CI, confidence interval.

Table S7. qPCR primer sequences used in this study.

Target (human)	Forward	Reverse
BRD2	CTACGTAAGAAACCCCGGAAG	GCTTTTTCTCCAAAGCCAGTT
BRD3	CCTCAGGGAGATGCTATCCA	ATGTCGTGGTAGTCGTGCAG
BRD4	AGCAGCAACAGCAATGTGAG	GCTTGCACTTGTCCTCTTCC
c-Myc	AGGGATCGCGCTGAGTATAA	TGCCTCTCGCTGGAATTACT
IL7R	TGTCGTCTATCGGGAAGGAG	CGGTAAGCTACATCGTGCATTA
FOXF2	CCGTTACCAGCATCACTCTACT	CGCAGGGCTTAATATCCTGACA
ACKR3	TACACGCTCTCCTTCATTTACA	AATGGCCAGGTTCAAGATGTAG
GPR68	TGTACCATCGACCATACCATCC	GGTAGCCGAAGTAGAGGGACA
SPOCD1	TCATACCTCAATGATAGGCAGC	CATCTTTTGAACCTTCCCCAAC
ANO1	GACTACCACGAGGATGACAAG	CATGGATTTTCACAAACCCGAC
VEGFC	ATTACAGTGCCTCTCTCTCAAG	CATCCAGTTTAGACATGCATCG
RAB3IL1	AGGAAGCTCACAAGATGGTTCG	GTGGACGTGATGACCAGTGT
BCAT1	GGATAGAATGTATCGCTCTGCT	AGGCTCAGTTCCAATGAATGTA
ANKRD2	GAGGCTCAACCGCTACAAAAT	CCTGCCAGGTTCTTGGTCATC
GAPDH	AGGTGAAGGTCGGAGTCAAC	AGTTGAGGTCAATGAAGGGG
18sRNA	ACACGGACAGGATTGACAGA	GGACATCTAAGGGCATCACA
FRMD5	CAAGCCAAGTCCGCACAGT	GCACTTGATTCCATGACTTCCTT
MXD4	GCACCAGTTGCTTGAGCTG	CAACGAGCTAGAAAAGCACAG
PITPNM3	GTTCCAAGCAGCAATCAGGT	TCACAATATCTCACCGTACACCA
TRIB3	AGGACTCCTGCGTGCTGACTG	AGGAGGCAGCGAACCAGACAG

Table S8. Antibodies used in this study.

Specificity	Source	Catalog number	Application (Concentration)
BRD4	Bethyl laboratories	A301-985A-M	IHC (1:200); WB (1:1000)
c-Myc	Cell Signaling	#9402	WB (1:1000)
Sox2	Cell Signaling	#3579	WB (1:1000)
Nanog	Cell Signaling	#4903	WB (1:1000)
Bmi1	Cell Signaling	#6964	WB (1:1000)
CD44	Cell Signaling	#3570	WB (1:1000)
CD133	Cell Signaling	#64326	WB (1:1000)
Cleaved PARP	Cell Signaling	#9541	WB (1:1000)
Cleaved Caspase3	Cell Signaling	#9664	IHC (1:200); WB (1:1000)
Bax	Cell Signaling	#5023	WB (1:1000)
Bcl-2	Cell Signaling	#2872	WB (1:1000)
E-cadherin	Cell Signaling	#14472	WB (1:1000)
N-cadherin	Cell Signaling	#13116	WB (1:1000)
Flag	Sigma	F3165	WB (1:2000)
Vimentin	GeneTex	GTX100619	WB (1:1000)
Ki-67	Abcam	ab15580	IHC (1:200)
c-Myc	Abcam	ab39688	IHC (1:200)
GAPDH	Santa Cruz	sc-47724	WB (1:500)
β-Actin	Santa Cruz	sc-58673	WB (1:500)

Figure S1

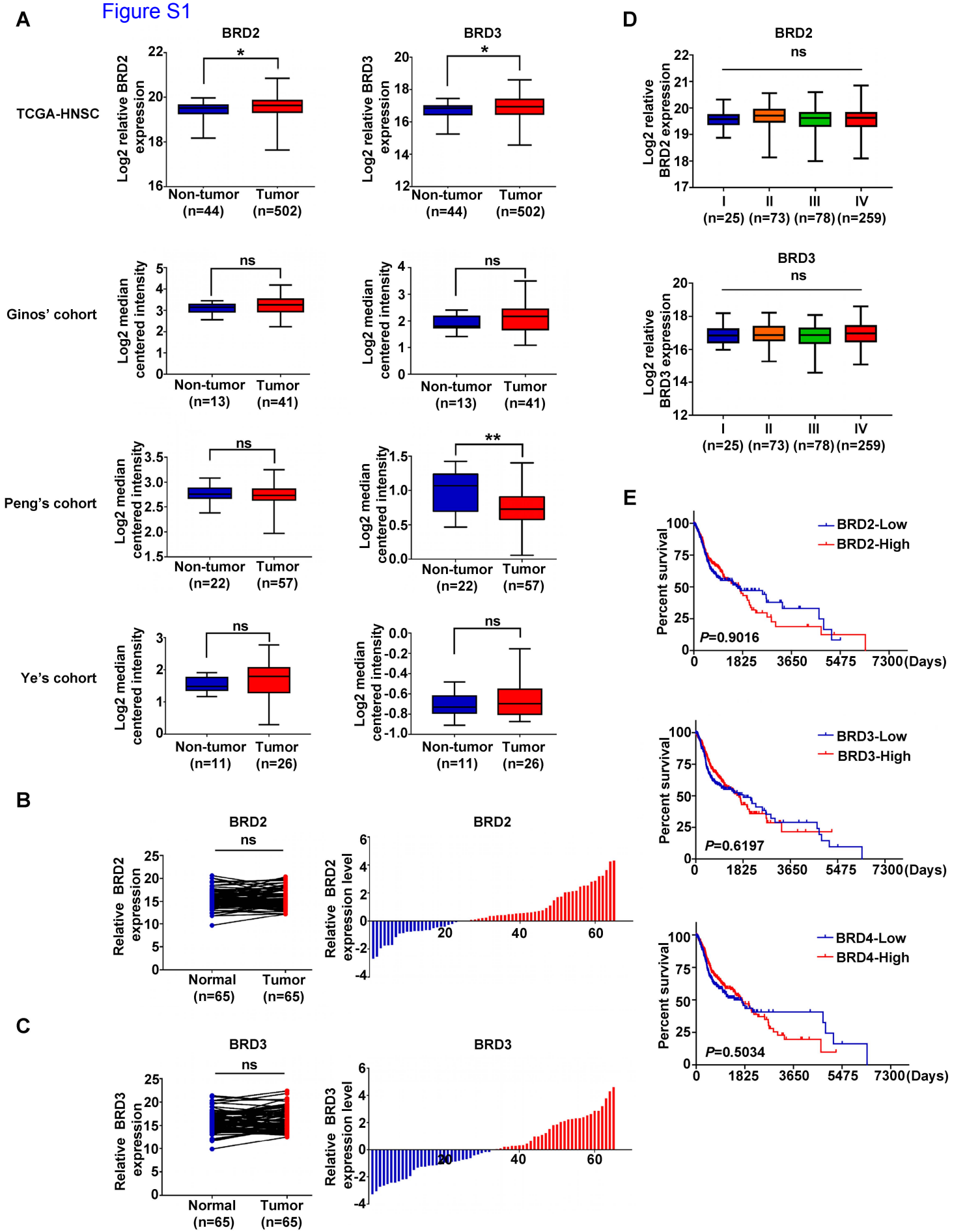
A
TCGA-HNSC
Ginos' cohort
Peng's cohort
Ye's cohort
BRD2
BRD3
Log2 relative BRD2 expression
Log2 relative BRD3 expression
Log2 median centered intensity
Non-tumor (n=44)
Tumor (n=502)
Non-tumor (n=13)
Tumor (n=41)
Non-tumor (n=22)
Tumor (n=57)
Non-tumor (n=11)
Tumor (n=26)
ns
*
**
B
C
Relative BRD2 expression
Relative BRD3 expression
Normal (n=65)
Tumor (n=65)
Relative BRD2 expression level
Relative BRD3 expression level
D
Log2 relative BRD2 expression
Log2 relative BRD3 expression
I (n=25)
II (n=73)
III (n=78)
IV (n=259)
E
Percent survival
BRD2-Low
BRD2-High
P=0.9016
BRD3-Low
BRD3-High
P=0.6197
BRD4-Low
BRD4-High
P=0.5034
0
1825
3650
5475
7300(Days)

Figure S2

A

cBioPortal FOR CANCER GENOMICS — Data Sets | Web API | R/MATLAB | Tutorials | FAQ | News | Visualize Your Data | About | Login

Modify Query — **Head and Neck Squamous Cell Carcinoma (TCGA, Provisional)**
All Complete Tumors (**496** samples) / **3** Genes

Gene Set / Pathway is altered in 125 (25.2%) of queried samples

OncoPrint | Cancer Types Summary | Mutual Exclusivity | Plots | Mutations | Co-Expression | Enrichments | Survival | Network | CN Segments | Download | Bookmark

Case Set: All Complete Tumors (496 patients / 496 samples)

Altered in 125 (25%) of 496 sequenced cases/patients (496 total)

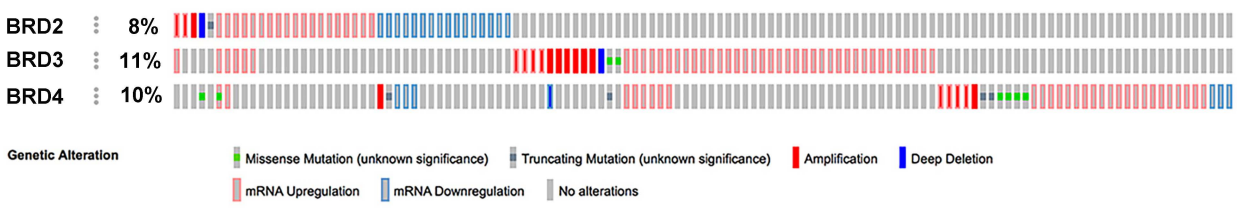

B

Modify Query — **Head and Neck Squamous Cell Carcinoma (TCGA, Provisional)**
All Complete Tumors (**496** samples) / **3** Genes

Gene Set / Pathway is altered in 125 (25.2%) of queried samples

OncoPrint | Cancer Types Summary | Mutual Exclusivity | Plots | Mutations | Co-Expression | Enrichments | Survival | Network | CN Segments | Download | Bookmark

BRD2 | BRD3 | BRD4

BRD2

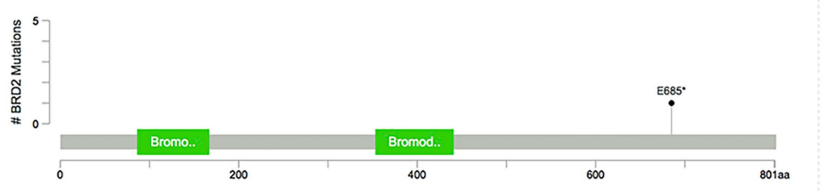

BRD2
UniProt: BRD2_HUMAN
Transcript: ENST00000374825
Somatic Mutation Frequency: 0.2%

0 Missense | 1 Truncating | 0 Inframe | 0 Other

View 3D Structure

1 Mutation (page 1 of 1)

Columns

Sample ID	Protein Change	Annotation ▼	Mutation Type	Copy #	COSMIC	Allele Freq (T)	# Mut in Sample
TCGA-CV-6956-01	*E685**		Nonsense	Diploid		0.06	161

Showing 1-1 of 1 Mutation

C

Modify Query — **Head and Neck Squamous Cell Carcinoma (TCGA, Provisional)**
All Complete Tumors (**496** samples) / **3** Genes

Gene Set / Pathway is altered in 125 (25.2%) of queried samples

OncoPrint | Cancer Types Summary | Mutual Exclusivity | Plots | Mutations | Co-Expression | Enrichments | Survival | Network | CN Segments | Download | Bookmark

BRD2 | BRD3 | BRD4

BRD3

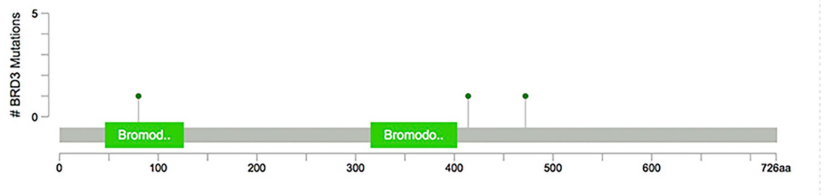

BRD3
Transcript: ENST00000303407
Somatic Mutation Frequency: 0.4%

3 Missense | 0 Truncating | 0 Inframe | 0 Other

View 3D Structure

3 Mutations (page 1 of 1)

Columns

Sample ID	Protein Change	Annotation ▼	Mutation Type	Copy #	COSMIC	Allele Freq (T)	# Mut in Sample
TCGA-DQ-5630-01	*P80L*		Missense	Diploid		0.07	75
TCGA-F7-A624-01	*K414R*		Missense	Diploid		0.15	3181
TCGA-F7-A624-01	*A472G*		Missense	Diploid		0.18	3181

Showing 1-3 of 3 Mutations

D

BRD2 | BRD3 | BRD4

BRD4

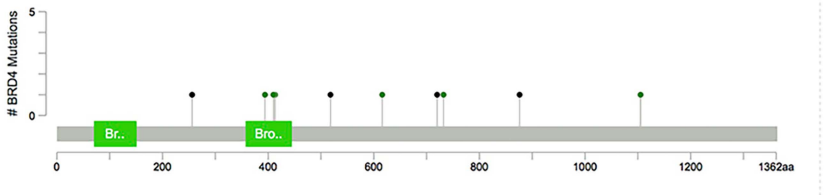

BRD4
UniProt: BRD4_HUMAN
Transcript: ENST00000263377
Somatic Mutation Frequency: 2.0%

6 Missense | 4 Truncating | 0 Inframe | 0 Other

View 3D Structure

10 Mutations (page 1 of 1)

Columns

Sample ID	Protein Change	Annotation ▼	Mutation Type	Copy #	COSMIC	Allele Freq (T)	# Mut in Sample
TCGA-CN-5370-01	*R410C*		Missense	ShallowDel		0.33	104
TCGA-BB-4223-01	*I394M*		Missense	Gain		0.04	296
TCGA-CN-5369-01	*R413H*		Missense	Diploid		0.09	455
TCGA-CQ-6221-01	*X720_splice*		Splice	Diploid		0.33	111
TCGA-CV-7261-01	*R616Q*		Missense	Gain		0.21	111
TCGA-MZ-A6I9-01	*G732R*		Missense	Diploid		0.06	42
TCGA-F7-A624-01	*Q256Sfs*27*		FS del	Diploid		0.25	3181
TCGA-BB-A5HY-01	*Q1105R*		Missense	ShallowDel		0.30	198
TCGA-CN-4726-01	*A877Sfs*40*		FS ins	Diploid		0.19	81
TCGA-CV-A6K2-01	*L518=*		Splice	Gain		0.16	599

Showing 1-10 of 10 Mutations

Figure S3

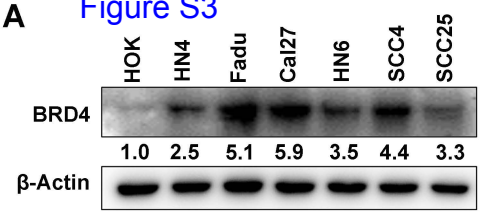
A
HOK
HN4
Fadu
Cal27
HN6
SCC4
SCC25
BRD4
1.0 2.5 5.1 5.9 3.5 4.4 3.3
β-Actin

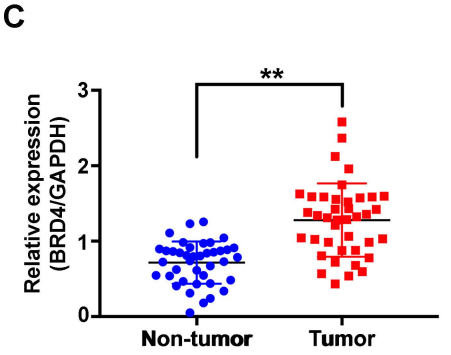
C
**
Relative expression (BRD4/GAPDH)
3
2
1
0
Non-tumor
Tumor

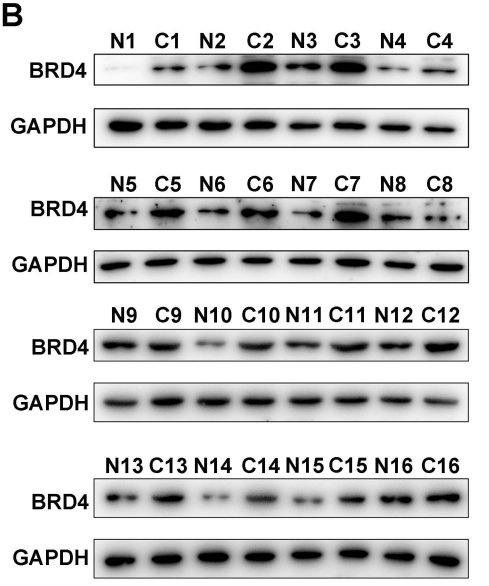
B
N1 C1 N2 C2 N3 C3 N4 C4
BRD4
GAPDH
N5 C5 N6 C6 N7 C7 N8 C8
BRD4
GAPDH
N9 C9 N10 C10 N11 C11 N12 C12
BRD4
GAPDH
N13 C13 N14 C14 N15 C15 N16 C16
BRD4
GAPDH

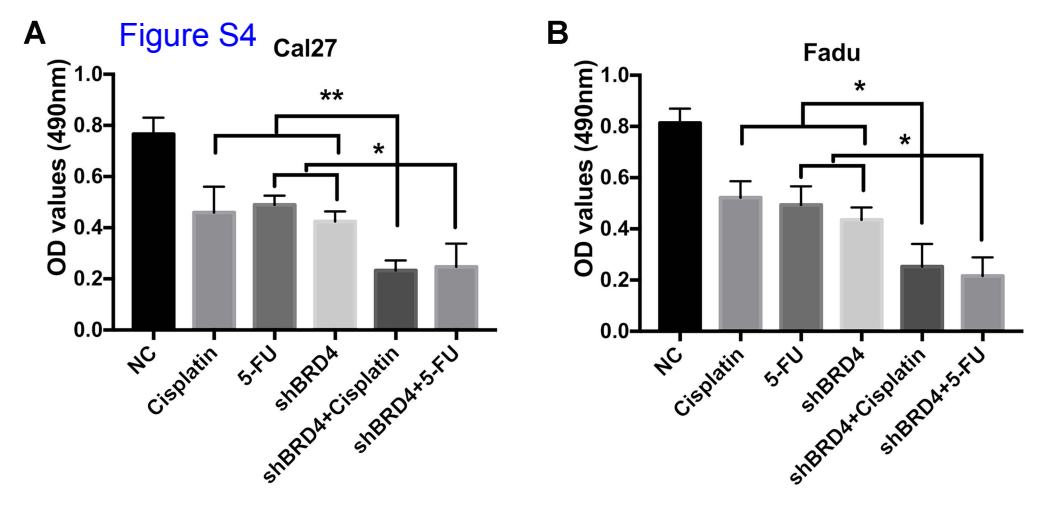
A
Figure S4
Cal27
OD values (490nm)
1.0
0.8
0.6
0.4
0.2
0.0
**
*
NC
Cisplatin
5-FU
shBRD4
shBRD4+Cisplatin
shBRD4+5-FU
B
Fadu
OD values (490nm)
1.0
0.8
0.6
0.4
0.2
0.0
*
*
NC
Cisplatin
5-FU
shBRD4
shBRD4+Cisplatin
shBRD4+5-FU

Figure S5

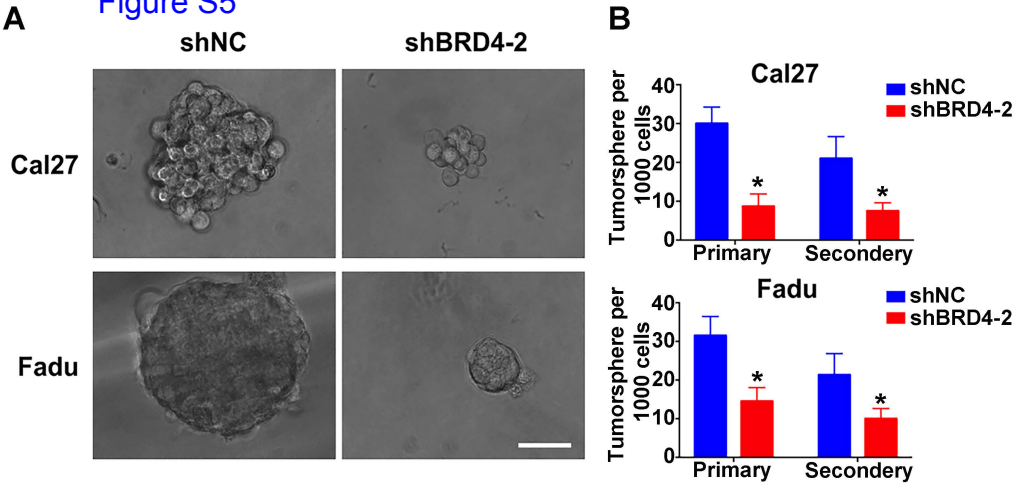
A
shNC
shBRD4-2
Cal27
Fadu
B
Cal27
shNC
shBRD4-2
Tumorsphere per 1000 cells
40
30
20
10
0
*
*
Primary
Secondery
Fadu
shNC
shBRD4-2
Tumorsphere per 1000 cells
40
30
20
10
0
*
*
Primary
Secondery

Figure S6

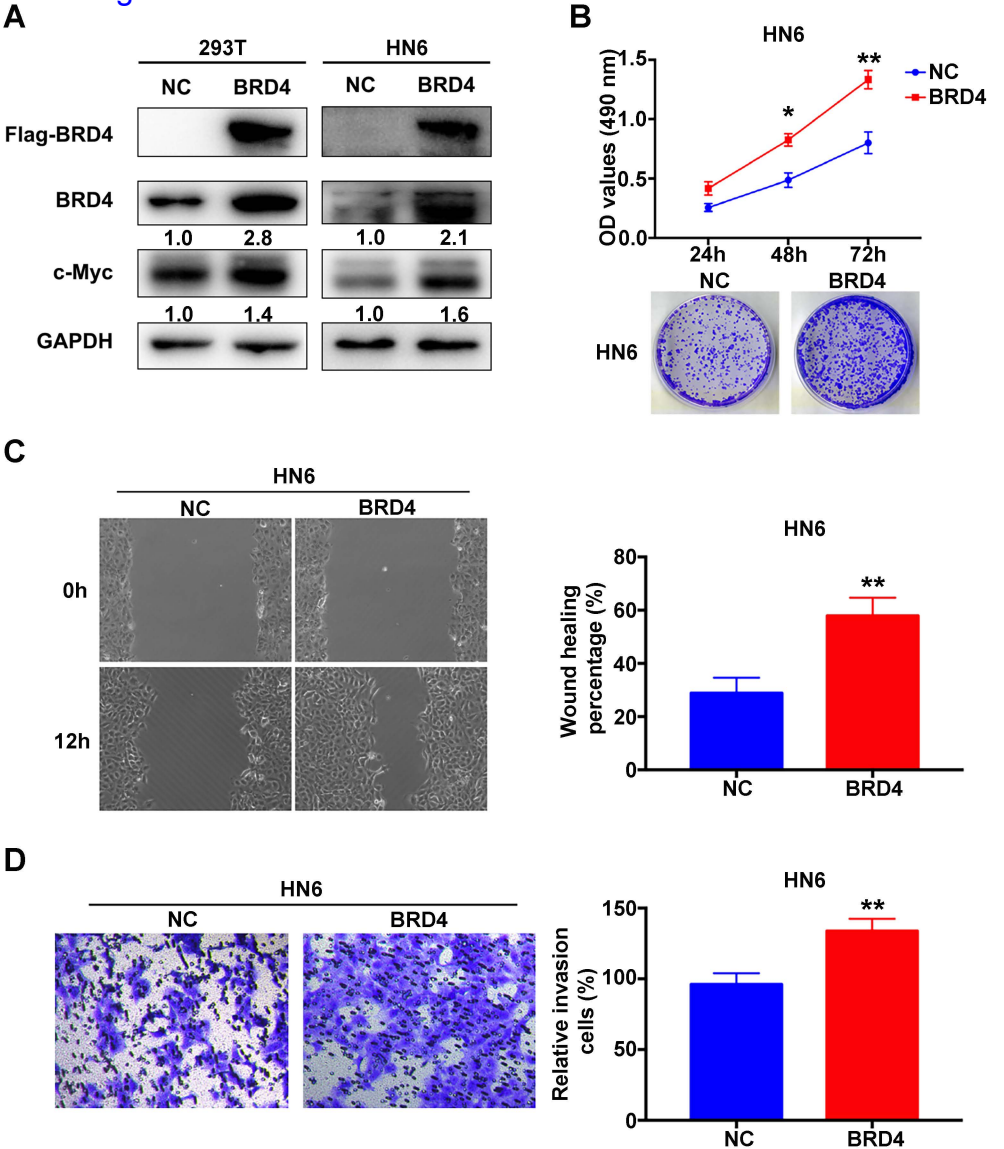
A
293T
HN6
NC
BRD4
NC
BRD4
Flag-BRD4
BRD4
1.0
2.8
1.0
2.1
c-Myc
1.0
1.4
1.0
1.6
GAPDH
B
HN6
OD values (490 nm)
1.5
1.0
0.5
0.0
*
**
NC
BRD4
24h
48h
72h
NC
BRD4
HN6
C
HN6
NC
BRD4
0h
12h
HN6
Wound healing percentage (%)
80
60
40
20
0
**
NC
BRD4
D
HN6
NC
BRD4
HN6
Relative invasion cells (%)
150
100
50
0
**
NC
BRD4

Figure S7

A

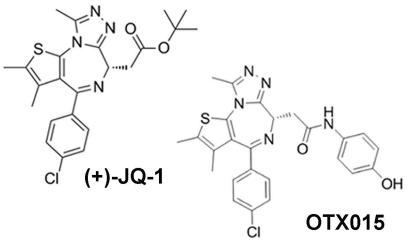

B

BET inhibitors IC50 (72h)		
Cell lines	JQ1	OTX015
Cal27	806.2nM	954.2nM
Fadu	615.3nM	841.7nM
BMSC	31633nM	99205nM
HOK	8746nM	10762nM

C

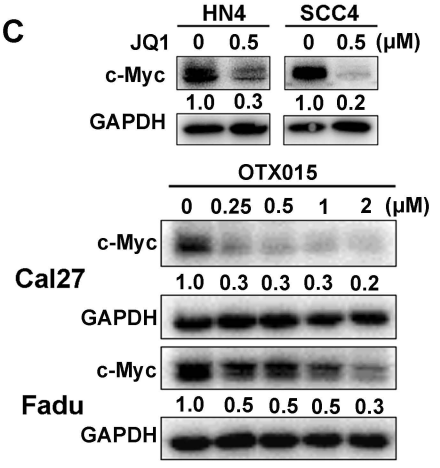

D

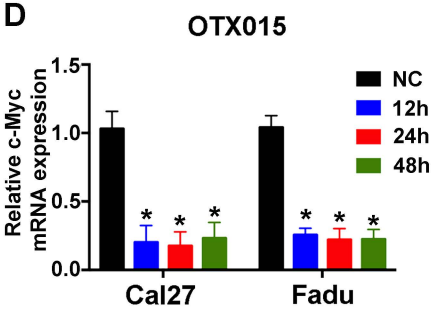

E

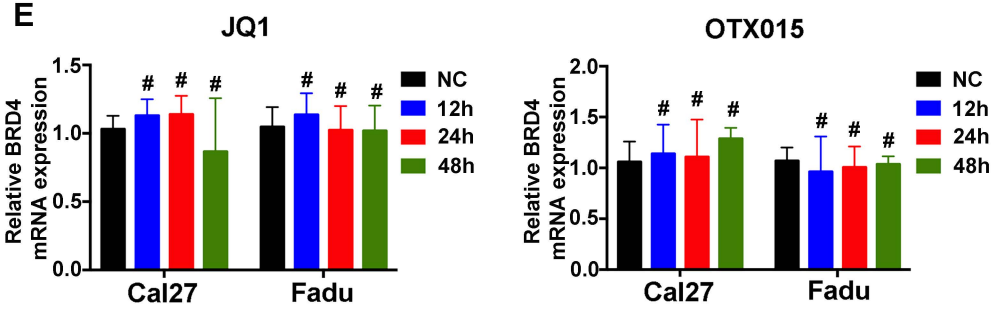

Figure S8

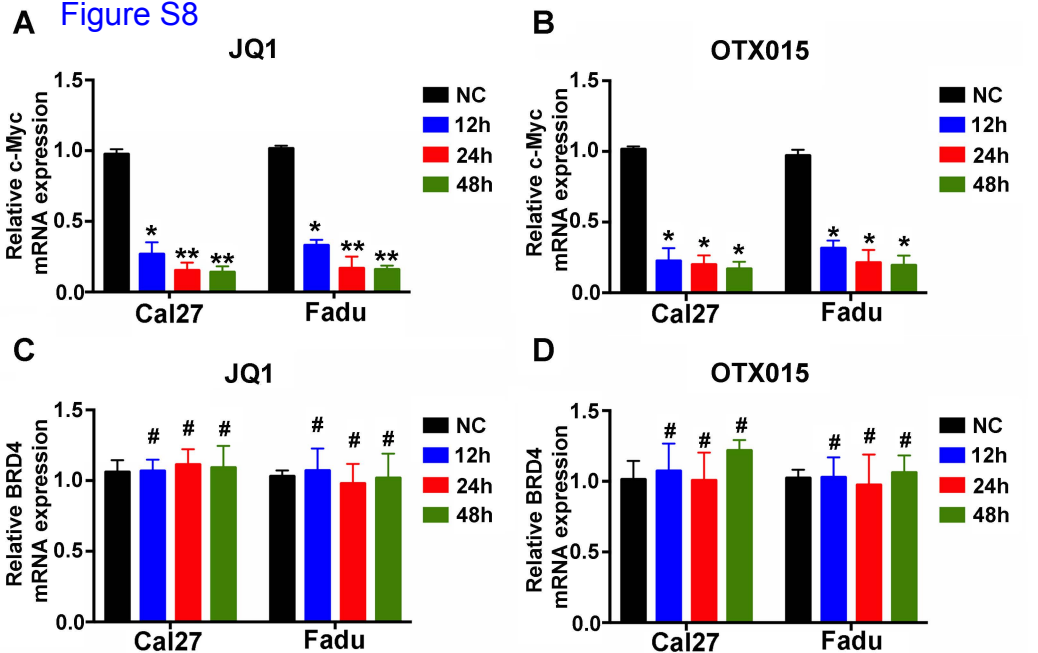
A
JQ1
Relative c-Myc mRNA expression
1.5
1.0
0.5
0.0
NC
12h
24h
48h
*
**
**
*
**
**
Cal27
Fadu
B
OTX015
Relative c-Myc mRNA expression
NC
12h
24h
48h
*
*
*
*
*
*
Cal27
Fadu
C
JQ1
Relative BRD4 mRNA expression
NC
12h
24h
48h
#
#
#
#
#
#
Cal27
Fadu
D
OTX015
Relative BRD4 mRNA expression
NC
12h
24h
48h
#
#
#
#
#
#
Cal27
Fadu

Figure S9

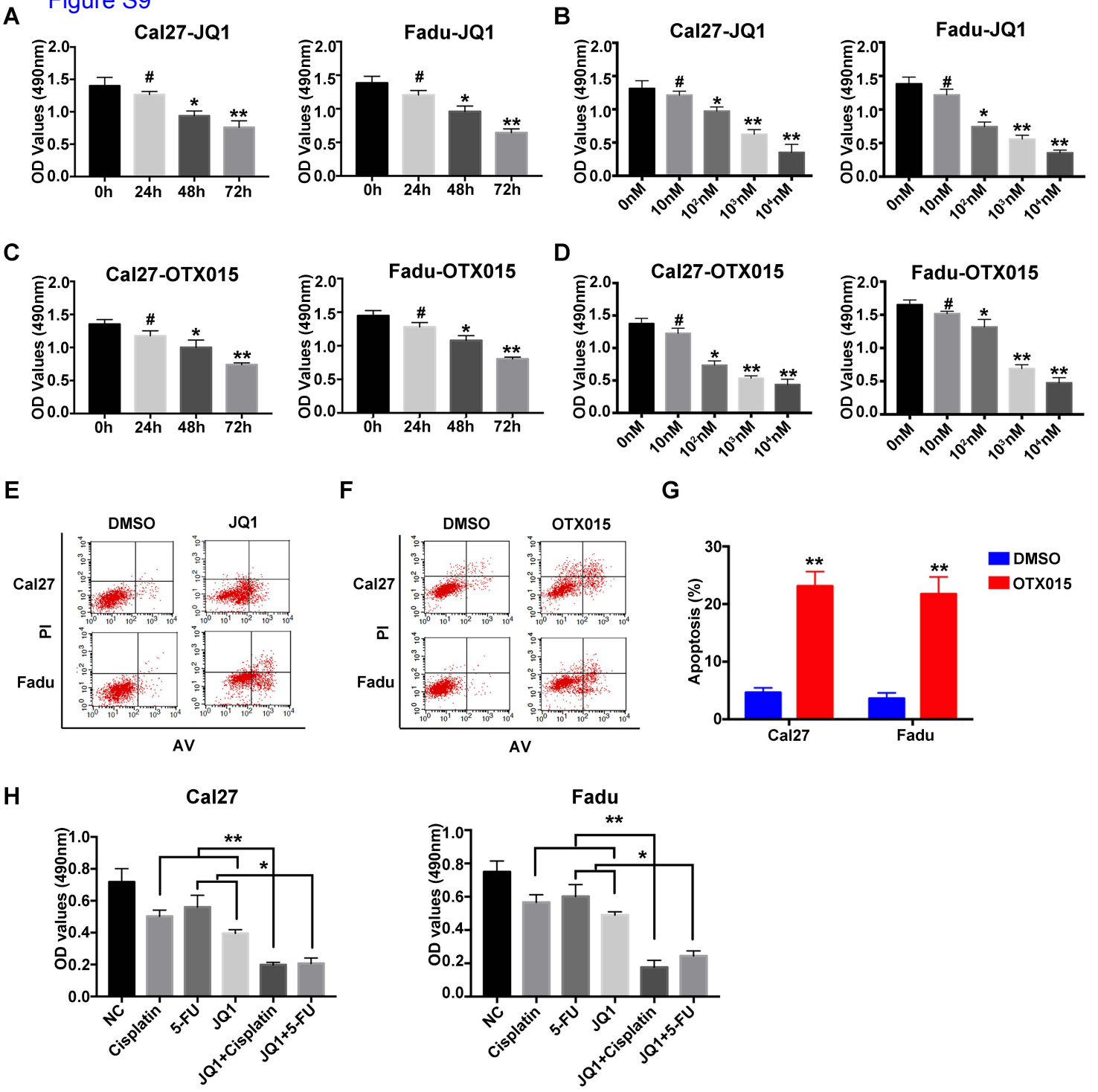
A
Cal27-JQ1
Fadu-JQ1
OD Values (490nm)
0h
24h
48h
72h
B
Cal27-JQ1
Fadu-JQ1
0nM
10nM
10²nM
10³nM
10⁴nM
C
Cal27-OTX015
Fadu-OTX015
D
Cal27-OTX015
Fadu-OTX015
E
DMSO
JQ1
Cal27
PI
Fadu
AV
F
DMSO
OTX015
G
Apoptosis (%)
DMSO
OTX015
Cal27
Fadu
H
Cal27
Fadu
OD values (490nm)
NC
Cisplatin
5-FU
JQ1
JQ1+Cisplatin
JQ1+5-FU

Figure S10

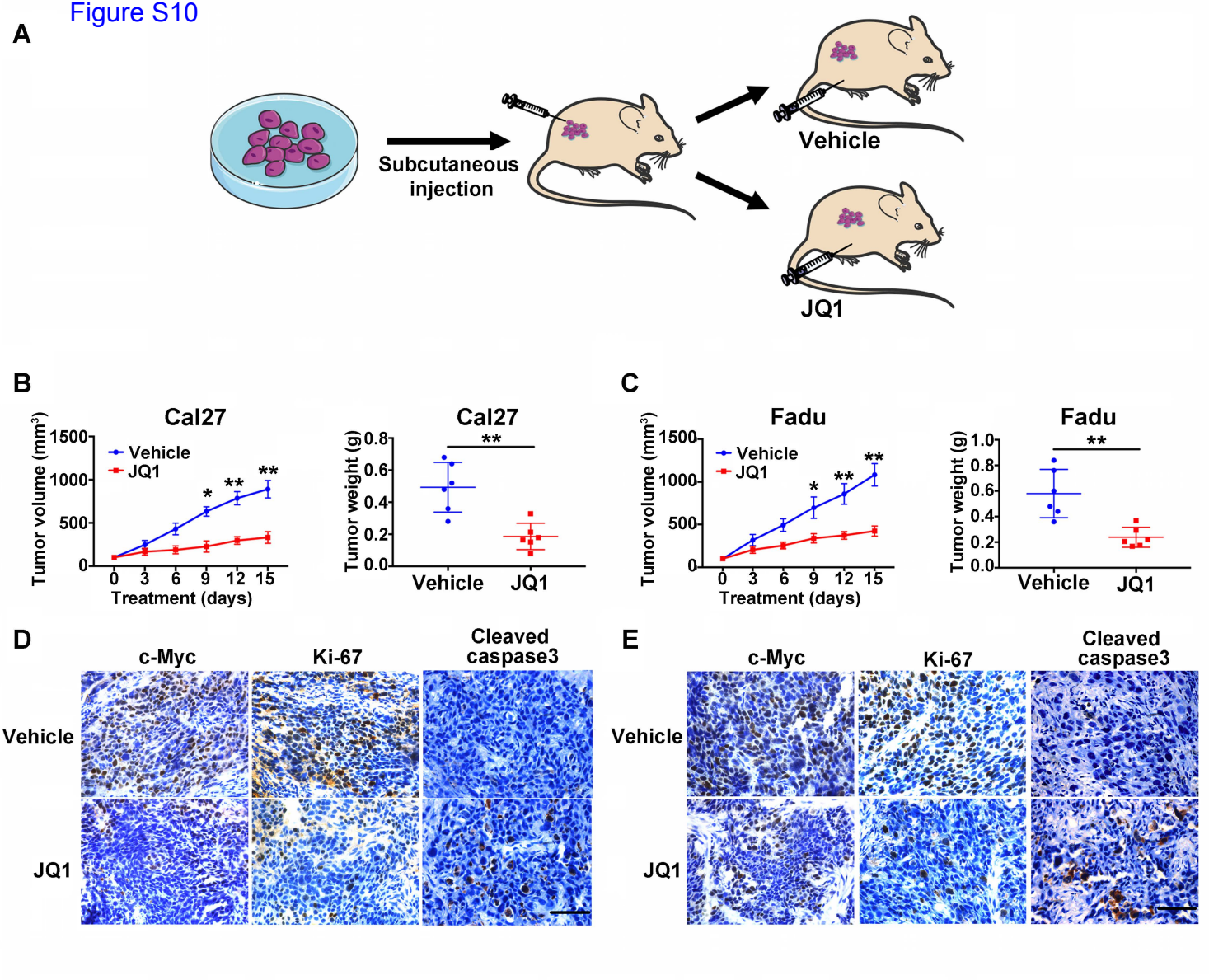
A
Subcutaneous injection
Vehicle
JQ1
B
Cal27
Tumor volume (mm3)
Vehicle
JQ1
Treatment (days)
Cal27
Tumor weight (g)
Vehicle
JQ1
C
Fadu
Tumor volume (mm3)
Vehicle
JQ1
Treatment (days)
Fadu
Tumor weight (g)
Vehicle
JQ1
D
c-Myc
Ki-67
Cleaved caspase3
Vehicle
JQ1
E
c-Myc
Ki-67
Cleaved caspase3
Vehicle
JQ1

Figure S11

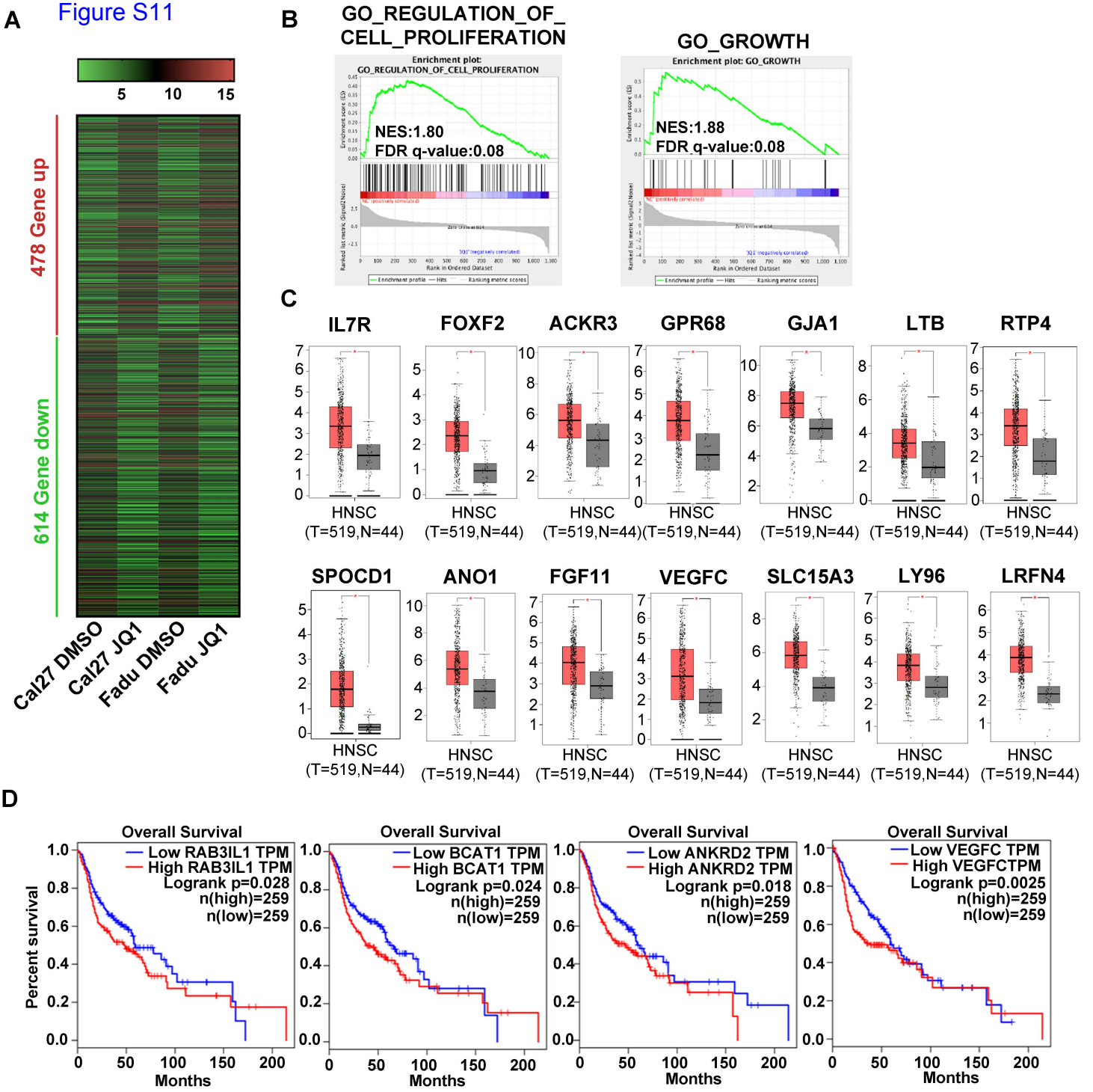
A
5
10
15
478 Gene up
614 Gene down
Cal27 DMSO
Cal27 JQ1
Fadu DMSO
Fadu JQ1
B
GO_REGULATION_OF_CELL_PROLIFERATION
Enrichment plot: GO_REGULATION_OF_CELL_PROLIFERATION
NES:1.80
FDR q-value:0.08
GO_GROWTH
Enrichment plot: GO_GROWTH
NES:1.88
FDR q-value:0.08
C
IL7R
FOXF2
ACKR3
GPR68
GJA1
LTB
RTP4
SPOCD1
ANO1
FGF11
VEGFC
SLC15A3
LY96
LRFN4
HNSC
(T=519,N=44)
D
Overall Survival
Low RAB3IL1 TPM
High RAB3IL1 TPM
Logrank p=0.028
n(high)=259
n(low)=259
Low BCAT1 TPM
High BCAT1 TPM
Logrank p=0.024
n(high)=259
n(low)=259
Low ANKRD2 TPM
High ANKRD2 TPM
Logrank p=0.018
n(high)=259
n(low)=259
Low VEGFC TPM
High VEGFCTPM
Logrank p=0.0025
n(high)=259
n(low)=259
Percent survival
Months

A Figure S12

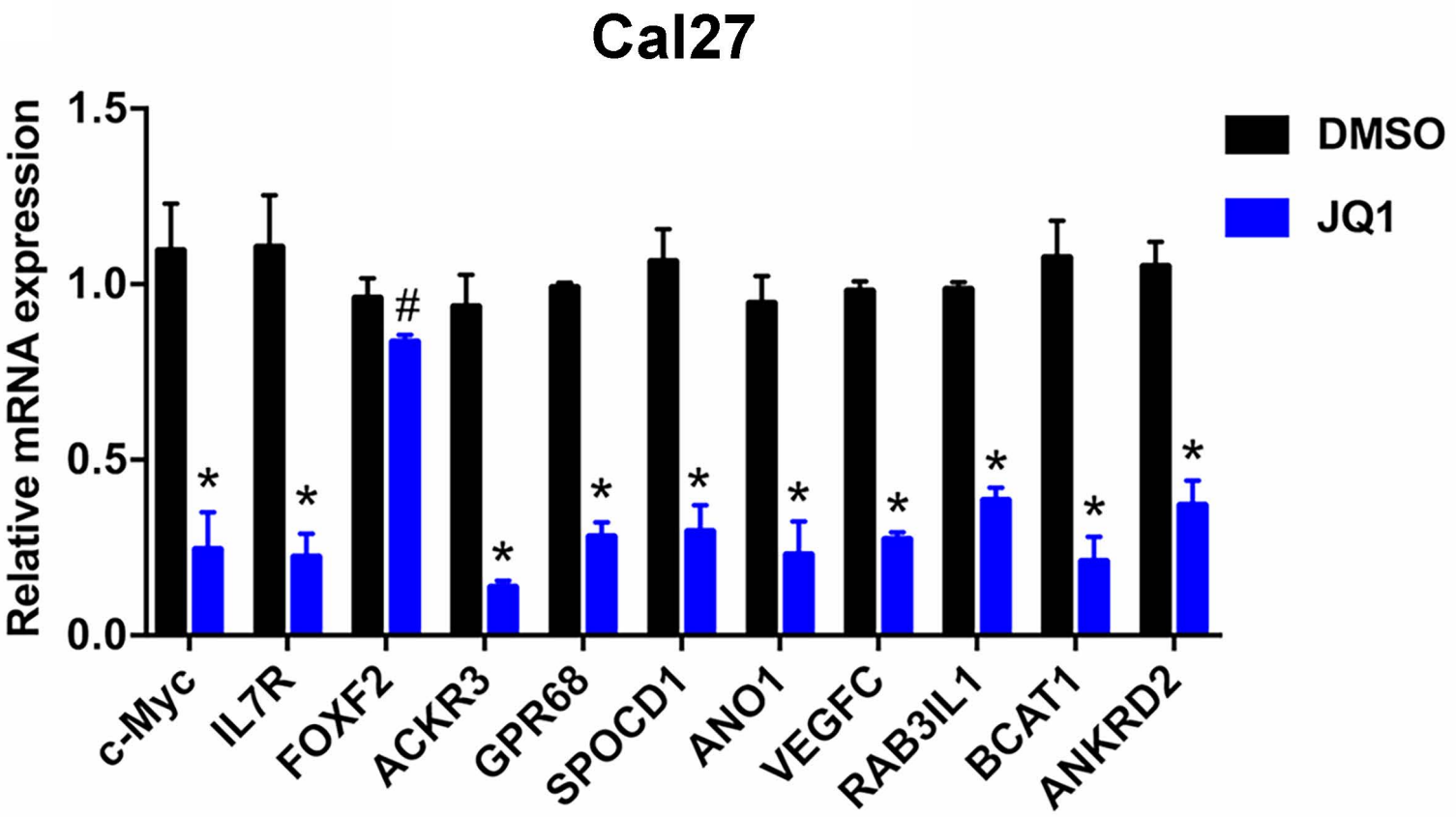

B

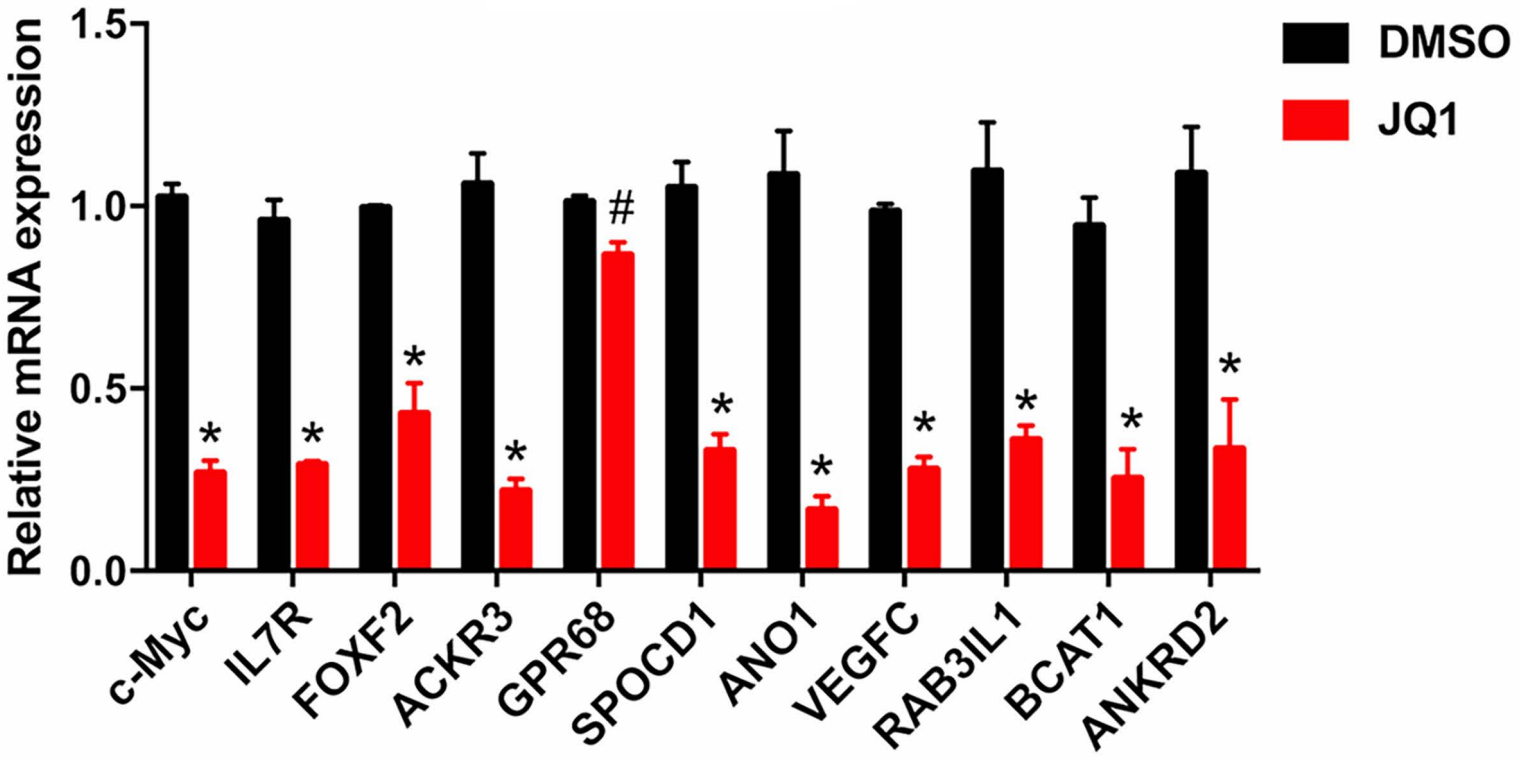

Figure S13

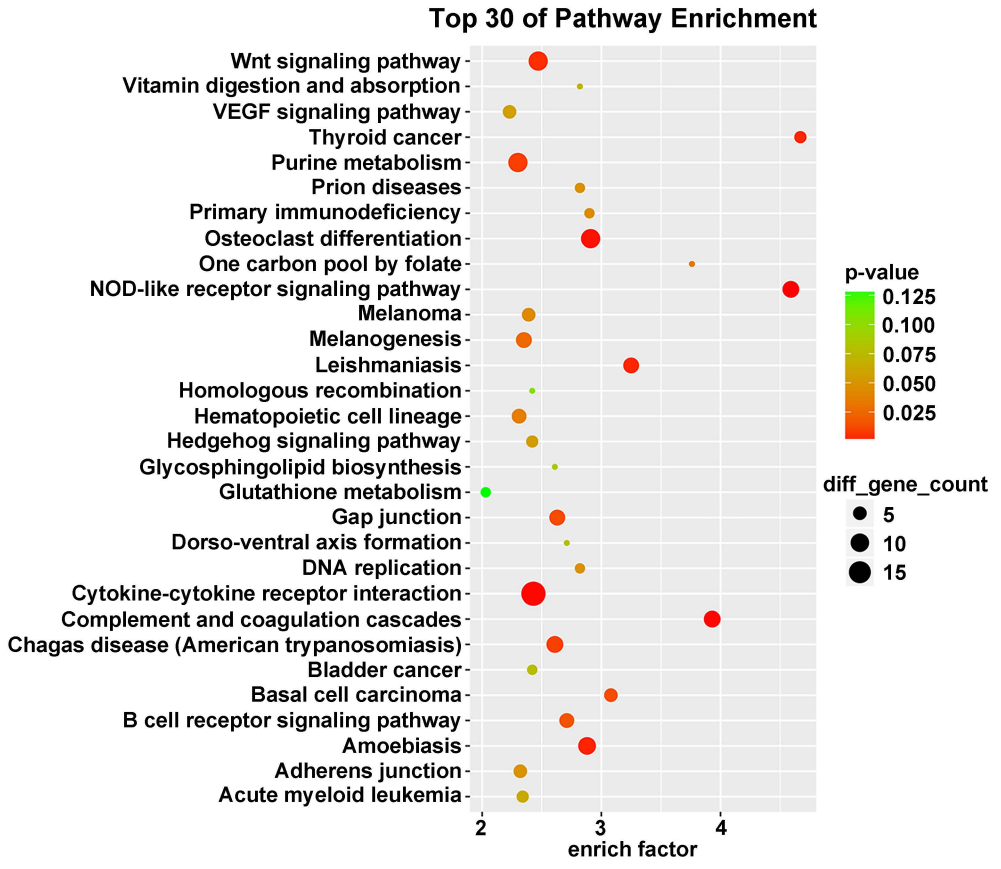
A
Top 30 of Pathway Enrichment
Wnt signaling pathway
Vitamin digestion and absorption
VEGF signaling pathway
Thyroid cancer
Purine metabolism
Prion diseases
Primary immunodeficiency
Osteoclast differentiation
One carbon pool by folate
NOD-like receptor signaling pathway
Melanoma
Melanogenesis
Leishmaniasis
Homologous recombination
Hematopoietic cell lineage
Hedgehog signaling pathway
Glycosphingolipid biosynthesis
Glutathione metabolism
Gap junction
Dorso-ventral axis formation
DNA replication
Cytokine-cytokine receptor interaction
Complement and coagulation cascades
Chagas disease (American trypanosomiasis)
Bladder cancer
Basal cell carcinoma
B cell receptor signaling pathway
Amoebiasis
Adherens junction
Acute myeloid leukemia
2
3
4
enrich factor
p-value
0.125
0.100
0.075
0.050
0.025
diff_gene_count
5
10
15

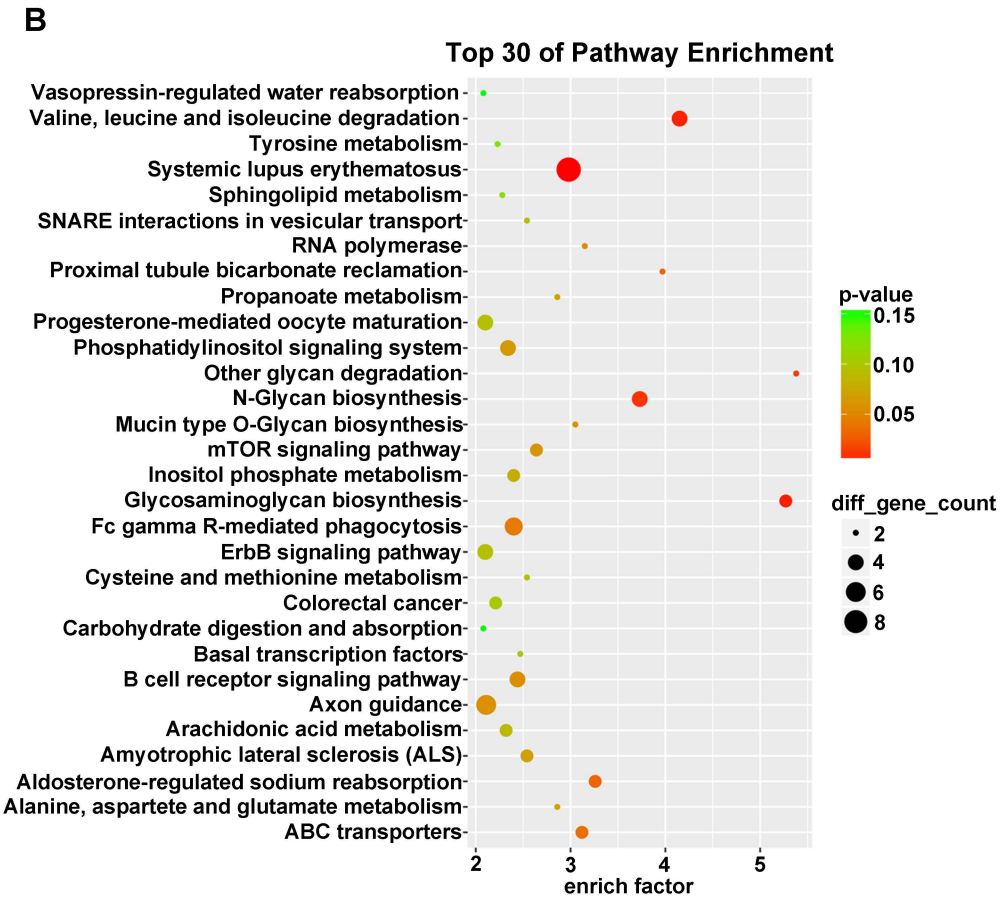
B
Top 30 of Pathway Enrichment
Vasopressin-regulated water reabsorption
Valine, leucine and isoleucine degradation
Tyrosine metabolism
Systemic lupus erythematosus
Sphingolipid metabolism
SNARE interactions in vesicular transport
RNA polymerase
Proximal tubule bicarbonate reclamation
Propanoate metabolism
Progesterone-mediated oocyte maturation
Phosphatidylinositol signaling system
Other glycan degradation
N-Glycan biosynthesis
Mucin type O-Glycan biosynthesis
mTOR signaling pathway
Inositol phosphate metabolism
Glycosaminoglycan biosynthesis
Fc gamma R-mediated phagocytosis
ErbB signaling pathway
Cysteine and methionine metabolism
Colorectal cancer
Carbohydrate digestion and absorption
Basal transcription factors
B cell receptor signaling pathway
Axon guidance
Arachidonic acid metabolism
Amyotrophic lateral sclerosis (ALS)
Aldosterone-regulated sodium reabsorption
Alanine, aspartete and glutamate metabolism
ABC transporters
2
3
4
5
enrich factor
p-value
0.15
0.10
0.05
diff_gene_count
2
4
6
8

Figure S14

A

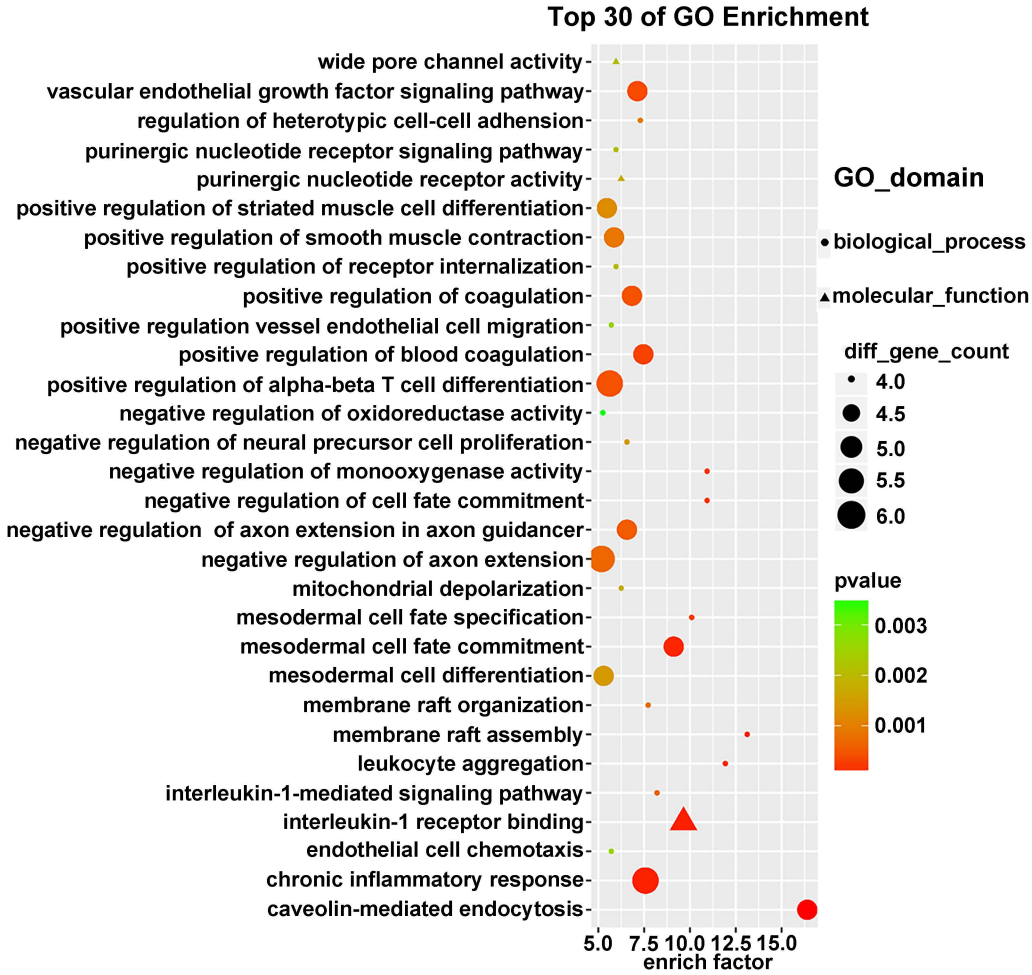

B

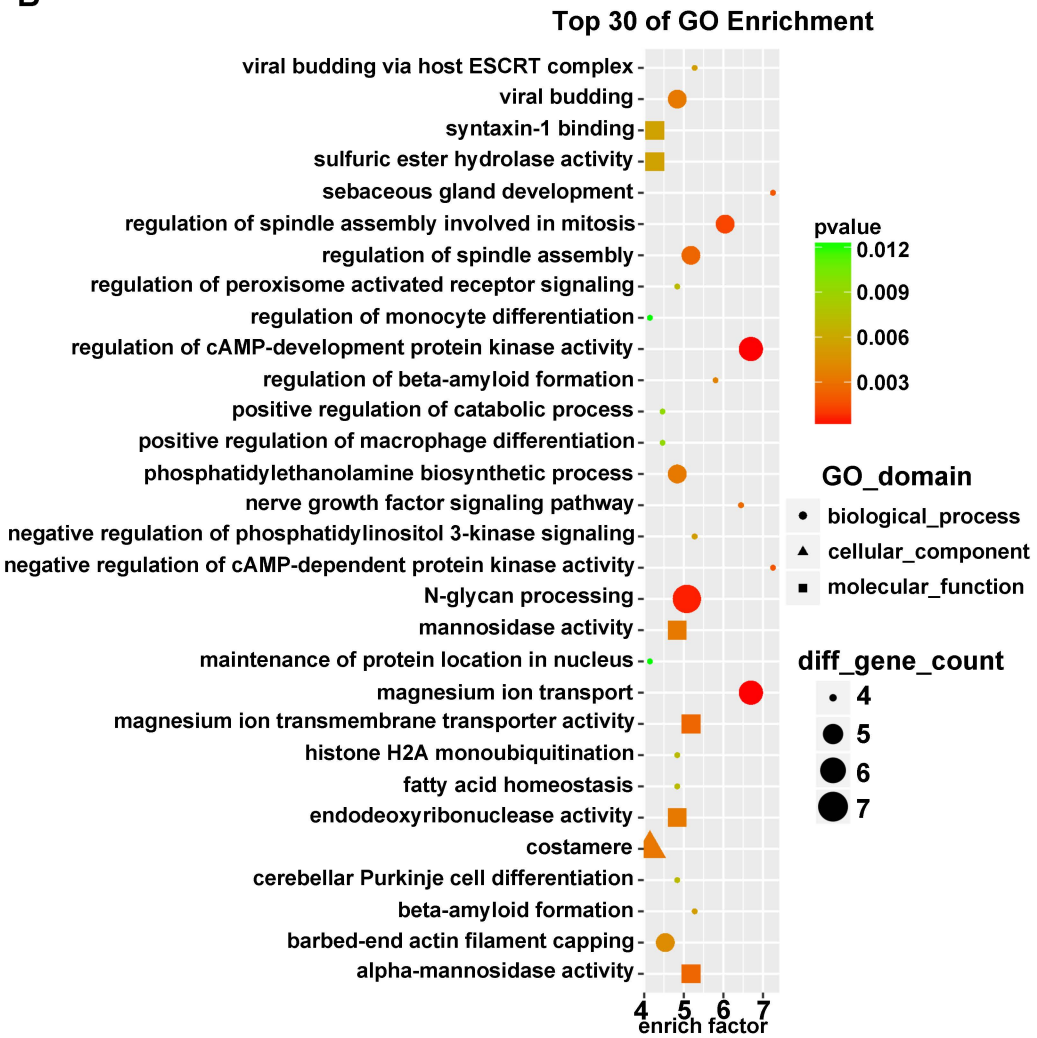

Figure S15

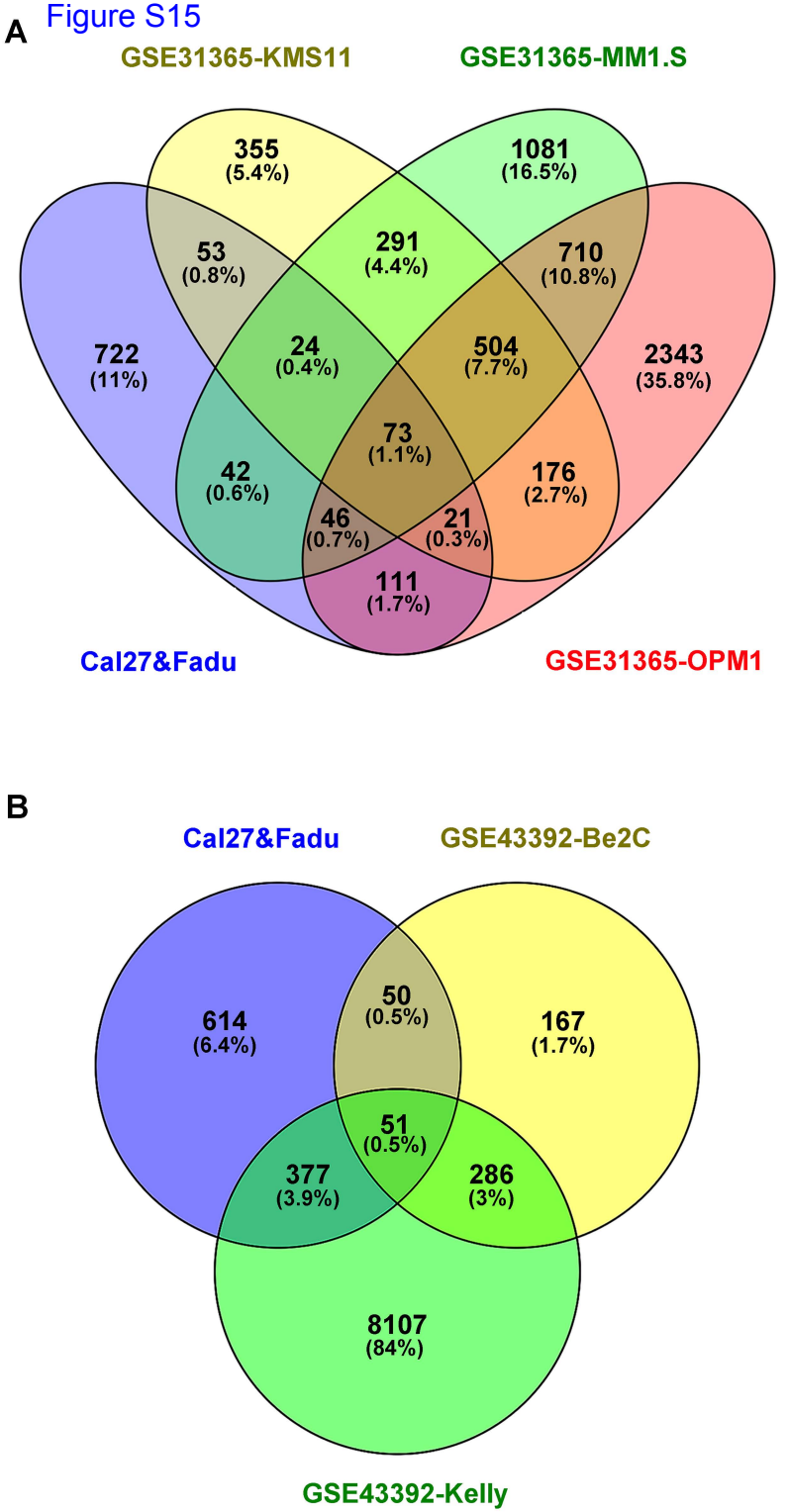
A
GSE31365-KMS11
GSE31365-MM1.S
355
(5.4%)
1081
(16.5%)
53
(0.8%)
291
(4.4%)
710
(10.8%)
722
(11%)
24
(0.4%)
504
(7.7%)
2343
(35.8%)
73
(1.1%)
42
(0.6%)
176
(2.7%)
46
(0.7%)
21
(0.3%)
111
(1.7%)
Cal27&Fadu
GSE31365-OPM1
B
Cal27&Fadu
GSE43392-Be2C
614
(6.4%)
50
(0.5%)
167
(1.7%)
51
(0.5%)
377
(3.9%)
286
(3%)
8107
(84%)
GSE43392-Kelly

Figure S16

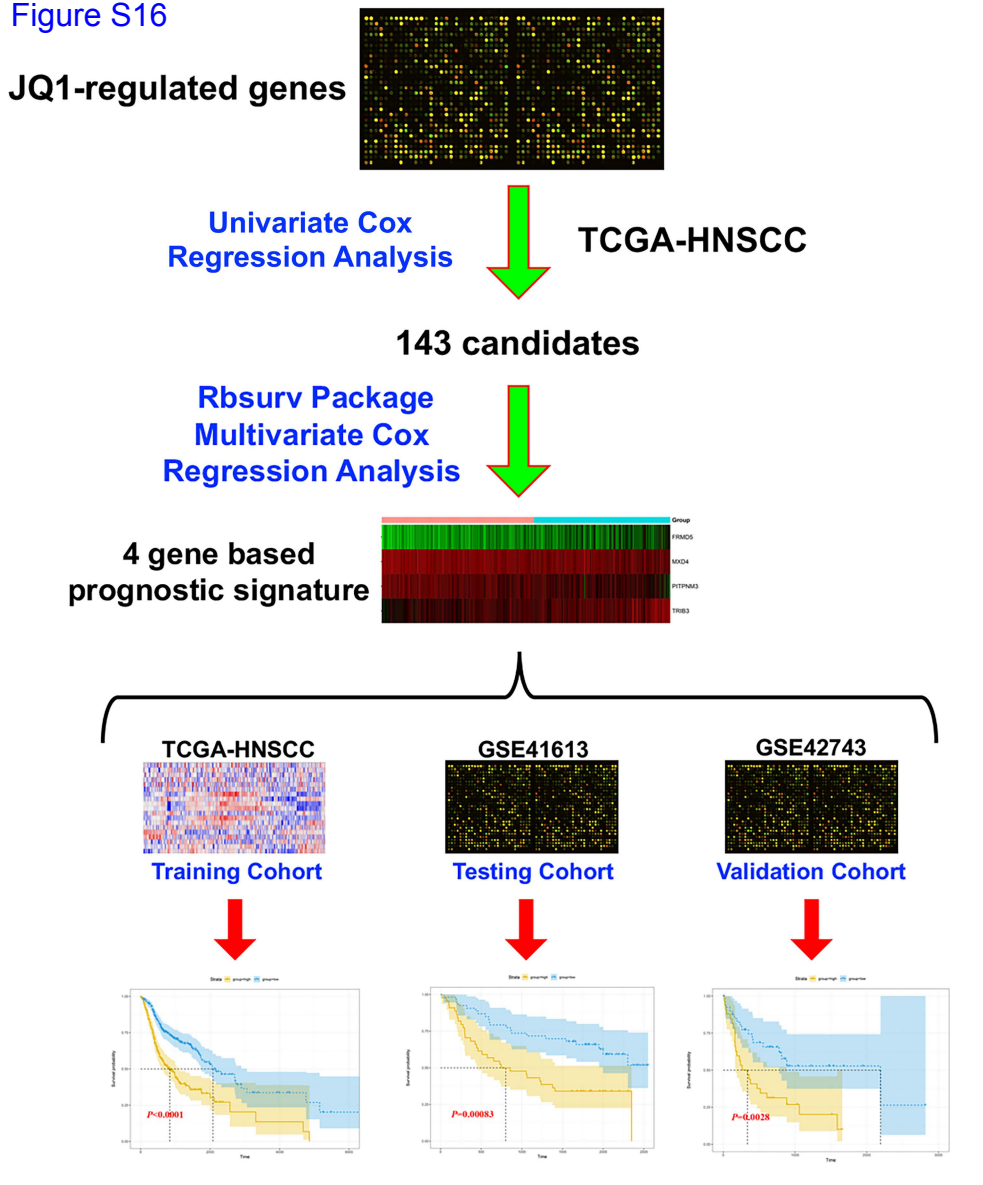
JQ1-regulated genes
Univariate Cox Regression Analysis
TCGA-HNSCC
143 candidates
Rbsurv Package Multivariate Cox Regression Analysis
4 gene based prognostic signature
Group
FRMD5
MXD4
PTPN13
TRIB3
TCGA-HNSCC
GSE41613
GSE42743
Training Cohort
Testing Cohort
Validation Cohort
P<0.0001
P=0.00083
P=0.0028

Figure S17

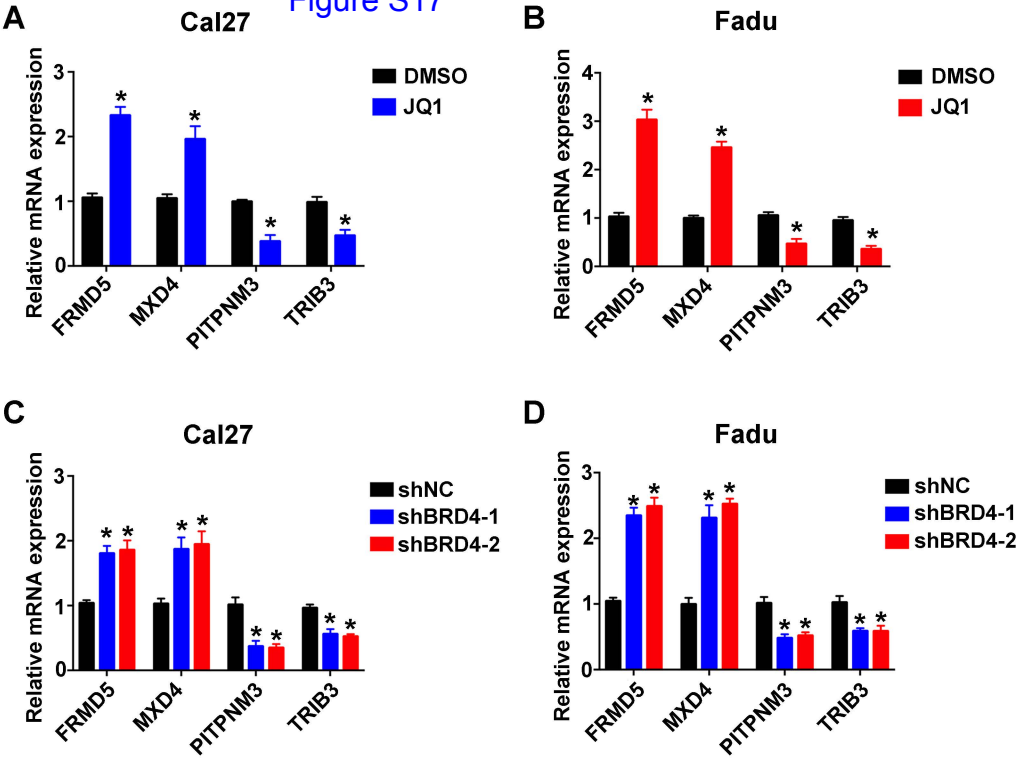
A
Cal27
Relative mRNA expression
DMSO
JQ1
FRMD5
MXD4
PITPNM3
TRIB3
B
Fadu
Relative mRNA expression
DMSO
JQ1
FRMD5
MXD4
PITPNM3
TRIB3
C
Cal27
Relative mRNA expression
shNC
shBRD4-1
shBRD4-2
FRMD5
MXD4
PITPNM3
TRIB3
D
Fadu
Relative mRNA expression
shNC
shBRD4-1
shBRD4-2
FRMD5
MXD4
PITPNM3
TRIB3

Figure S18

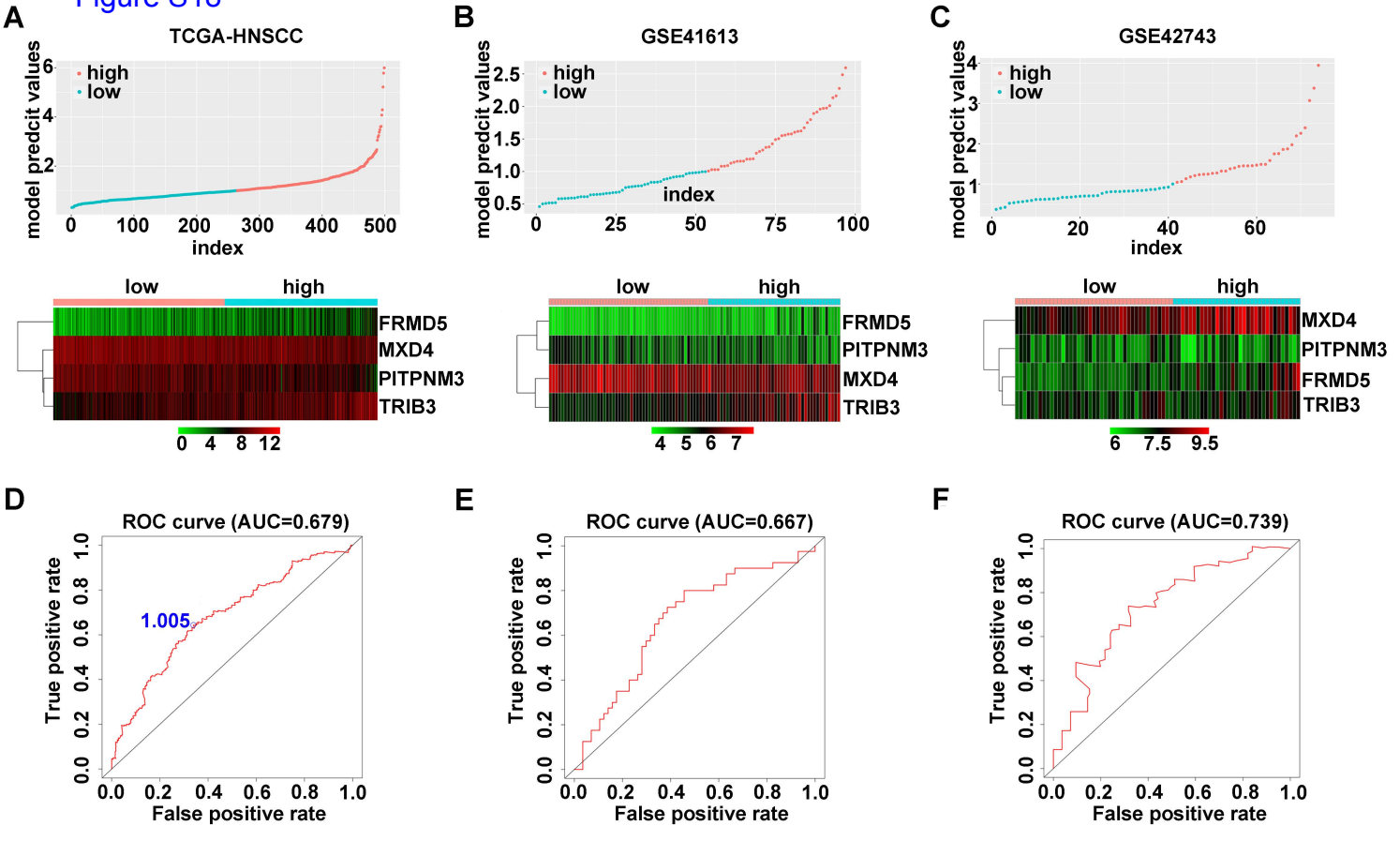
A
TCGA-HNSCC
model predcit values
high
low
index
low
high
FRMD5
MXD4
PITPNM3
TRIB3
B
GSE41613
C
GSE42743
D
ROC curve (AUC=0.679)
1.005
True positive rate
False positive rate
E
ROC curve (AUC=0.667)
F
ROC curve (AUC=0.739)